Available online at www.sciencedirect.com
ScienceDirect
Ceramics International 35 (2009) 1919–1926
CERAMICS INTERNATIONAL
www.elsevier.com/locate/ceramint

Processing and impact behavior of Al/SiCp composites fabricated by the pressureless melt infiltration method

A.M. Zahedi [a], H.R. Rezaie [a,*], J. Javadpour [a], Mehdi Mazaheri [b,**], M.G. Haghighi [a,b]

[a] *Faculty of Materials and Metallurgical Engineering, Iran University of Science and Technology (IUST), Tehran, Iran*
[b] *Materials and Energy Research Center (MERC), P.O. Box 14155-477, Tehran, Iran*

Received 28 May 2008; received in revised form 10 September 2008; accepted 20 October 2008
Available online 17 November 2008

Abstract

In the current investigation, pressureless melt infiltration was applied to fabricate the Al/SiC composites based on the SiC porous preforms. The process was conducted by introducing the aluminum melt into the SiC preforms at 950 °C under the nitrogen atmosphere, without the aid of pressure. To explore development of melt infiltration, initial preforms were produced with variable SiC fractions (40, 50, and 60 vol.%) using three different SiC powders with the mean particle size of 20, 50, and 90 μm. While the infiltration of aluminum melt into the preforms with 40 vol.% initial SiC volume fraction (SiC particle size of 90 μm) resulted to the composites with final density of 0.94 theoretical density (TD), this value drops down to ∼0.9 TD for the composites produced by preforms with the SiC (90 μm) volume fraction of 60 vol.%. On the other hand, composites fabricated by 50 μm SiC powder (SiC volume fraction of 40 vol.%) demonstrated the final density of ∼0.91 TD. The impact resistance tests performed on the composites demonstrated an enhancement in the value of impact energy with an increase of SiC powder particle size. Results, additionally, revealed a significant superiority of impact energy for the composites fabricated by a combined melt infiltration and sintering (MIS) procedure compared to those produced by infiltration at 950 and 1350 °C.
© 2008 Elsevier Ltd and Techna Group S.r.l. All rights reserved.

Keywords: B. Composite; Melt infiltration; Preform; Density

1. Introduction

The great interest that ceramic matrix composites (CMCs) have attracted through the recent decade stems from the combined effects of metallic and ceramic materials relative to the corresponding monolithic alloy. Excellent characteristics of these composites such as high-strength and modulus as well as good high-temperature properties have offered these materials as promising candidates for automotive and aerospace applications [1,2].

Aluminum composites based on the SiC preforms are among the most well-known CMCs, efficiently, applicable in technology due to their properties such as high-modulus, high-specific stiffness, high-temperature resistance, low-coefficient of thermal expansion, good workability and wear resistance. In addition to the numerous methods initiated to fabricate Al/SiC composites like stir casting and powder metallurgy, melt infiltration has, recently, appeared as an economic technique. This process involves penetration of Al melt into the pores of SiC preforms so as to make a ceramic–metal composite by taking the advantage of liquid state routes [1–3]. The obstacle of this process is, however, the non-wetting nature of SiC substrate by the aluminum melt, which results in weak ceramic–metal interfaces and incomplete infiltration. To assist the infiltration process, therefore, an external pressure or vacuum has to be applied to exceed the threshold pressure (P_0), i.e. the pressure required to overcome capillary back pressure [4–6]. Several researches [1,3,5–9] have, already, investigated employing an external pressure in fabricating Al/SiC composites by the melt infiltration process. Martins et al. [10], for example, developed a model based on the bundle of capillary tubes as an analogue for infiltration of SiC compacts by aluminum melt. Candan et al. [3] enforced the

* Corresponding author at: Faculty of Materials and Metallurgical Engineering, Iran University of Science and Technology (IUST), Narmak, Tehran, Iran.
** Corresponding author at: Swiss Federal Institute of Technology in Lausanne (EPFL) SB-IPMC-LNNME, PH D2 434 CH-1015 Lausanne, Switzerland. Tel.: +41 21 693 3389; fax: +41 21 633 4470.
E-mail addresses: sohrab.zahedi@gmail.com (A.M. Zahedi), hrezaie@iust.ac.ir (H.R. Rezaie), mehdi.mazaheri@epfl.ch (M. Mazaheri).

0272-8842/$34.00 © 2008 Elsevier Ltd and Techna Group S.r.l. All rights reserved.
doi:10.1016/j.ceramint.2008.10.024

aluminum melt into the SiC porous bodies and explored the role of surface tension of the Al melt in relation to the interface contact angle. They also demonstrated the effect of process parameters such as alloying additions to the aluminum melt [7] as well as infiltration temperature and time [5,6] on the evolution of infiltration procedure.

Contrary to the above-mentioned issues, numerous investigations [1,4,11,12] have, recently, focused on the pressureless infiltration of the Al melt into the pores of SiC preforms. The term ''pressureless infiltration'' describes the process by which the voids in the porous body are filled by the liquid metal without the aid of any external pressure [1,11]. However, there are some barriers that prevent this method to display its potential as a feasible technique of composite manufacturing. Paramount of these problems is the slight wetting of the SiC substrate by molten aluminum which is resulted from the formation of oxide layer on the surface of Al melt. Undesirable reactions at the Al/SiC interface are the other obstacle, altering the chemical composition of the molten aluminum and lead to the formation of unwanted phases at the interface, such as Al_4C_3 and Al_3SiC_4 [12].

Pech-Canul et al. [1,11] believe that optimum conditions are to be provided in order that a successful infiltration may be accomplished without using any artificial outer pressure. According to their comments, these optimum conditions include: (1) adding preferably more than 3% magnesium to the aluminum melt, (2) using SiC particles with a thin silicon wafer on the top, (3) providing the internal pressure of 1.2 atm for the furnace, and (4) changing the internal atmosphere of the furnace to 100% nitrogen [11]. Magnesium is a powerful surfactant that scavenges oxygen from the melt surface and forms the $MgAl_2O_4$ spinel at the Al/SiC interface. In addition to increasing the driving force for wetting, the reaction of producing $MgAl_2O_4$ spinel consumes the oxygen present in the atmosphere, thins the oxide layer, and thus enhances wetting [13,14]. Besides, application of nitrogen atmosphere not only hinders formation of the oxide layer but also enhances wetting of SiC by Al melt [11].

On the other hand, combined melt infiltration and sintering (MIS) method has been, recently, initiated to manufacture composites with a high-tensile ductility and the probability to attain ductile phase-toughened composites. Some investigations [15–18] have already, reported preparation of Ni_3Al/TiC composites using this procedure, which leads to an enhanced potential structural and wear applications. The MIS method, besides, is capable of providing high-density materials with an extended compositional range for the tough reinforcing phase. Reports concerning with production of Ni_3Al/TiC as well as FeAl/TiC composites are available in the literature [19–21]. Plucknett and Becher [22] studied melt infiltration, sintering, and grain growth behavior of MIS-processed Ni_3Al/TiC composites. They have managed to develop a densified Ni_3Al-toughened composite with a homogeneous microstructure in which the tough phase contents vary over the range of 4–25 vol.% [22]. In the present work, however, MIS has been applied to produce silicon carbide-based composites with a higher volume fraction of the aluminum (40–60 vol.%) as a tough phase in the final composite.

In addition to the application of MIS method as a novel process to fabricate Al/SiC composites, the current research is aimed at investigating the effect of SiC particle size (20, 50, and 90 μm) and initial density of preforms (0.4, 0.5, and 0.6 theoretical densities), separately, and in relation with each other on the development of pressureless infiltration process.

2. Experimental procedure

2.1. Raw materials

Silicon carbide (SiC) powder was purchased (Carborex, Germany), in three mean particle sizes of 20, 50, and 90 μm. Fig. 1 shows the scanning electron micrographs (SEM) of the utilized SiC powder in three particle sizes. The aluminum (Al) alloy used in this research has been Al–3 wt.% Mg, the chemical composition of which is represented in Table 1.

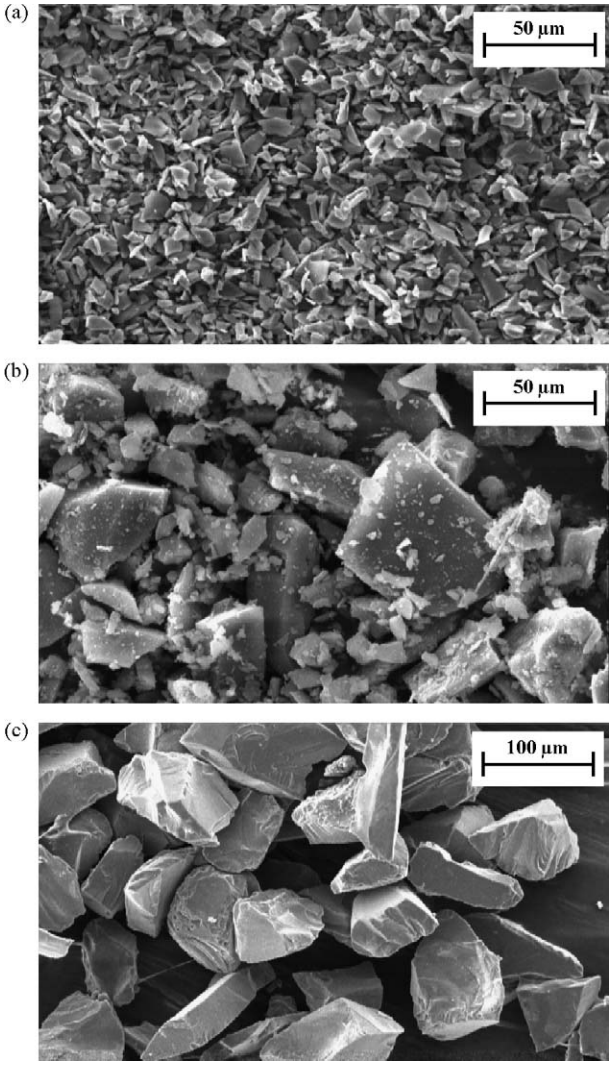

Fig. 1. Scanning electron micrographs (SEM) of SiC powders with (a) 20 μm, (b) 50 μm, and (c) 90 μm mean particle size.

Table 1
Chemical analysis of the applied Al–3 wt.% Mg alloy.

Al	97
Mg	3
Ti	0.01
Mn	0.04
Cu	0.008
Ni	0.005
Fe	0.09
Si	0.07
Zn	0.01
Cr	0.01

2.2. Composite fabrication

In order to produce SiC preforms, the powders of three particle sizes were mixed with 5 wt.% molten paraffin as the binder, and then the mixture was uniaxially cold pressed to the pellets of 12.7 mm diameter in steel die under a range of 100–700 MPa (Fig. 2). Due to the weakness of green bodies, density assessments were not performed on green bodies. Note that infiltration procedure has been carried out based on the sintered preforms with a definite amount of porosity indicated by sintered density of preforms. Thus, green density assessment has not been an influential factor on the output of the current work.

To remove the paraffin binder, the SiC green bodies (obtained by pressing) were heated to 300 °C for 30 min. Further, to obtain the preforms with 0.4, 0.5, and 0.6 theoretical densities (TD), pellets were heated with the rate of 10 °C min^{-1} to 1350 °C and soaked for 3 h. Density assessment of the sintered preforms was performed using the Archimedes method, regarding the SiC theoretical density as 3.21 g cm^{-3}. Fig. 2 demonstrated the sintered densities of preforms versus compaction pressure. Using diagrams, the optimized pressures for yielding porous preforms with the initial density of 0.4, 0.5, and 0.6 TD were obtained. Actually, the initial density of preforms, in the present work, is the same as the SiC volume fraction in the final density of composites. Fig. 3 shows the cross-section micrographs of the SiC preforms (0.5 TD initial density) employed in the infiltration process. In addition to the necking of SiC powder (due to the initial stage of sintering), connected pore channels can be seen in the figure through which the aluminum melt penetrates during the following melt infiltration procedure.

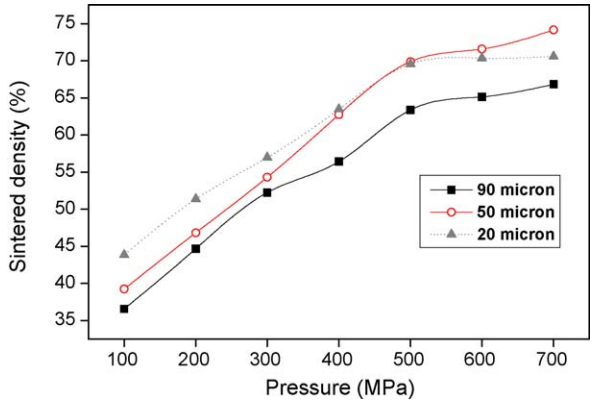

Fig. 2. Sintered density percentage of SiC porous preforms fabricated by 20, 50, and 90 μm SiC particle sizes as a function of compaction pressure.

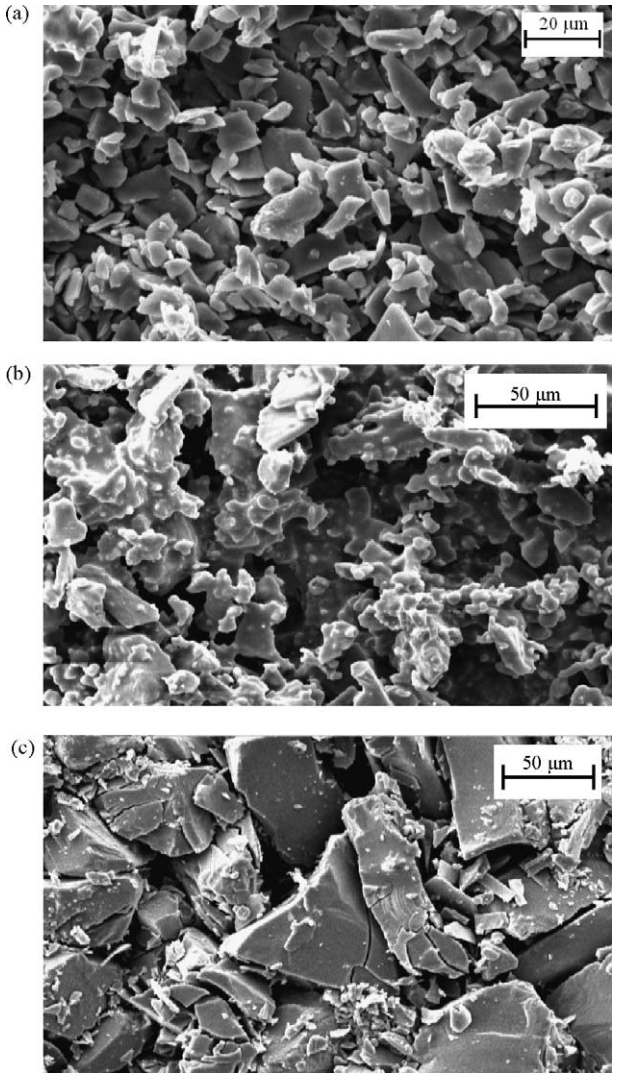

Fig. 3. Scanning electron microscopy (SEM) micrographs of SiC porous preforms (0.5 TD) fabricated by SiC powders with (a) 20 μm, (b) 50 μm, and (c) 90 μm particle size.

To infiltrate molten aluminum alloy into the voids of compacts, SiC preforms together with two 10 g cubes of the alloy, one on the top and the other under the SiC preform, were put in an alumina die, previously coated with boron nitride. Infiltration of these preforms with the alloy was performed in a tube furnace with an alumina tube that was closed at both ends. As both end fittings were sealed, a vacuum of 10^{-4} torr was maintained in the furnace before running the infiltration process. Preforms were, then, heated up to 950 °C with the rate of 10 °C min^{-1} and soaked for 75 min in the nitrogen atmosphere.

2.3. Characterization

In order to have an accurate density assessment (to eliminate the effects of surface contaminants such as boron nitride), the

specimens were mechanically polished after the infiltration procedure, to remove up to 1 mm from all sides of the pellets. Final density of composites was calculated using the Archimedes method. Based on the rule of mixture, theoretical density of composites with 40%, 50%, and 60% SiC volume fraction or 0.4, 0.5, and 0.6 TD initial density was determined to be 2.93, 2.98, and 3.04 g cm^{-3}, respectively. For each data point at least five samples have been tested. For investigating microstructural evolution, melt infiltrated composites were cut and the cross-section was mechanically polished. To study microstructural development of the composite, scanning electron microscopy (SEM, Philips XL30, The Netherlands) was used. Phase characterization of the ultimate composites fabricated by 90 μm SiC powder was performed using the X-ray diffraction (XRD) analysis (Philips, X'Pert, The Netherlands).

2.4. Impact energy

The impact resistance energy of composites was determined using charpy test based on the application of ASTM, E23. The mentioned powder mixture was, therefore, pressed to the specimens with the dimensions of 55 mm × 10 mm × 10 mm through the same pressure range. After achieving preforms with 0.4, 0.5, and 0.6 TD initial density (explained in Section 2.2) the specimens were processed using procedures mentioned in Table 2. To explore the influence of powder particle size on the impact energy of composites, porous preforms fabricated by 20, 50, and 90 μm SiC powder were introduced to the aluminum melt at 950 °C for 210, 150, and 105 min, respectively, under the nitrogen atmosphere (MI1). Longer infiltration times for finer powders was because of providing composites with near values of final density so as to eliminate the effect of density or retained microstructural porosity in the determination of impact energy values. Application of a higher infiltration temperature (1350 °C) in MI2 procedure (Table 2) was due to shed light on the effect of higher final densities (resulted from higher infiltration temperature) on the value of impact energy. To investigate the effect of combined melt infiltration and sintering process, the MIS procedure was conducted based on the conditions embedded in Table 2. After infiltration at 950 °C, composites were separated from the infiltration set-up and the atmosphere changed to Ar through heating the specimens up to 1350 °C with the rate of 10 °C min^{-1}.

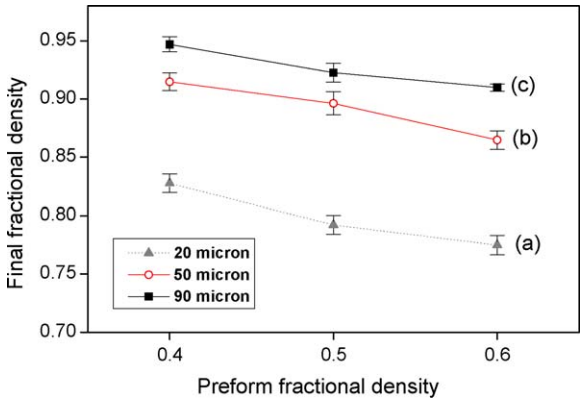

Fig. 4. Final fractional density of the Al/SiC composites as a function of preform initial density.

3. Results and discussion

Results related to the final density of all fabricated composites are displayed in Fig. 4 as a function of the preform initial density. As can be seen, increasing the initial density of preforms has resulted to a tangible decrease in the final densities of composites made by three different SiC powders. While the preforms made by 90 μm SiC powder with the initial density of 0.6 TD have the lowest value of composite final density (0.9 TD) among the preforms of curve (c), this value ascends to the highest amount for that of 0.4 TD (0.94 TD). The same trend can be seen for other diagrams of Fig. 4, as well. The other consequence is the improvement of composite densities with an increase in the SiC particle size. According to Fig. 4, while diagram (a) which reflects the obtained final density of composites produced based on the SiC powder with 20 μm particle size shows the lowest value, diagram (c) shows the highest final densities for the composites made on the preforms with 90 μm particle size powder. As mentioned, presence of a capillary back pressure called threshold pressure (P_0) in the infiltration process acts as a parameter to hinder the easy filling of the pores by the aluminum melt. To exert a proper infiltration process, therefore, either an external pressure is needed to

Table 2
Details of processing conditions for fabrication of impact energy specimens.

Procedure	*d* (μm)		
	90 Infiltration	50 Infiltration	20 Infiltration
MI1[a]	At 950 °C for 105 min in N_2	At 950 °C for 150 min in N_2	At 950 °C for 210 min in N_2
MI2[b]	At 1350 °C for 105 min in N_2	–	–

Procedure	*d* (μm)			
	90 Infiltration	90 Sintering	50 Infiltration	20 Infiltration
MIS[c]	At 950 °C for 105 min in N_2	At 1350 °C for 180 min in Ar	–	–

[a] Melt infiltration at 950 °C.
[b] Melt infiltration at 1350 °C.
[c] Melt infiltration at 950 °C + sintering at 1350 °C.

exceed P_0, or the optimum conditions of pressureless melt infiltration must be provided. The capillary pressure can be calculated using the following equation [1,3,5]:

$$P_0 = \frac{2\gamma_{lv}}{r}\cos\theta \quad (1)$$

where γ_{lv} is the liquid–vapor surface tension, θ is the contact angle at the liquid/solid interface and r is the capillary radius. This can be inferred from Eq. (1) that the threshold pressure changes with the inverse of capillary radius. Larger capillary radius, thus, leads to a lower threshold pressure for infiltration. Additionally, Carman [23] have proposed another parameter called hydraulic radius (r_h) which is defined through the following relation [1]:

$$r_h = \frac{r}{2} \quad (2)$$

Details of hydraulic radius are available in the literature [23]. Combining Eqs. (1) and (2) can be led to another equation by which the threshold pressure is directly related to the hydraulic radius [1,5,6]:

$$P_0 = \frac{\gamma_{lv}}{r_h}\cos\theta \quad (3)$$

Using Eq. (3), one can realize that every parameter to influence the hydraulic radius is definitely impressive on the threshold pressure. Candan et al. [5] represented a relation to recognize the effect of ceramic particle size (d) and initial volume fraction (initial density) of preforms (V_p) on the value of hydraulic radius:

$$r_h = \frac{(1 - V_p)d}{6V_p} \quad (4)$$

According to the above relation, decreasing V_p results to a rise in the value of r_h and that is why the preforms with the initial density of 0.4 TD enjoy the highest final density among the composites fabricated by three SiC particle sizes. This reason holds true for the effect of particle size as well. As can be seen in Fig. 5, hydraulic radius can boost when the SiC particle size increases. The fact is that, manufacturing composites based on the preforms of 90 μm SiC can be helpful to diminish the threshold pressure and consequently eases the infiltration of Al melt into the voids.

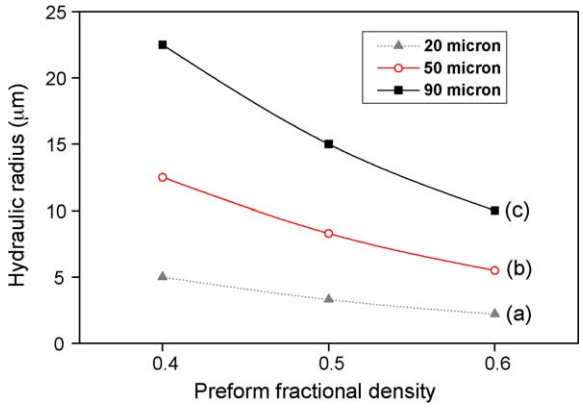

Fig. 5. Variation of hydraulic radius as a function of preform initial density.

Such an output is in full accordance with the data reported by Candan et al. [5]. They have come to this conclusion that a decrease in particle size lengthens the time needed for an equal amount of infiltration. In order to represent a credible analysis, Fig. 5 shows the trend of hydraulic radius variations as a function of preform initial density for different SiC particle sizes. The values corresponded to the hydraulic radius (Fig. 5) have been calculated using Eq. (4). While r_h = 22.5 μm for 0.4 TD dense preforms (90 μm), this value drops down to 10 μm for the preforms with 0.6 TD initial density (90 μm). The hydraulic radius for 0.4 TD dense preforms made by 50 μm SiC powder has been obtained to be 12.5 μm and final densities of composites verify the accuracy of above discussion.

The other considerable factor is the percentage of final density improvement by the infiltration of molten aluminum into the SiC compacts. Quote to the data displayed in Table 3, while the mentioned percentage for 0.4 TD dense preforms (90 μm) touched the highest value of 54%, such preforms fabricated by 20 μm SiC powder experienced not more than a 42% evolution. Considering the initial density of preforms as the variable factor, remarkable percentage of density enhancements, as mentioned, is the other explicit observation, taken place in return of a decrease in initial density (Table 3). However, the most significant task in Table 3 is the prevailing role of SiC volume fraction (preform initial density) in the evolution of melt infiltration process, compared to the SiC particle size. Contrary to the expectations, in spite of a smaller particle size related to 0.4 TD preforms of 20 μm SiC powder, these preforms managed to increase composite density to a higher extent of 42% rather than 0.5 and 0.6 TD preforms of 50 μm powder (39% and 26%, respectively). There are also other examples of such observation available in Table 3. This issue is well confirmed by Eq. (4) as well. As can be seen, reduction in V_p (SiC volume fraction) increases the numerator and declines the denominator of the fraction simultaneously, which leads to a remarkable increase in the value of hydraulic radius compared to particle size by which only the numerator of the fraction is effected.

The scanning electron microscopy micrographs of composite (0.4 TD dense preforms) microstructures are shown in Fig. 6. As can be seen in the images, the lowest amount of pores can be detected in the composite manufactured on the preforms of 90 μm SiC powder (Fig. 6c). The melt infiltration process conducted on the preforms made by 20 μm powder has demonstrated highest percentage of porosity (Fig. 6a) which are resulted from weak infiltration of the Al melt into the SiC compacts.

Table 3
The amount of composite final density progression compared to the original SiC preform in determined V_p (SiC volume fraction) and d (SiC particle size).

d (μm)	V_p		
	0.4 (TD)	0.5 (TD)	0.6 (TD)
20	0.427	0.292	0.174
50	0.514	0.396	0.264
90	0.547	0.423	0.309

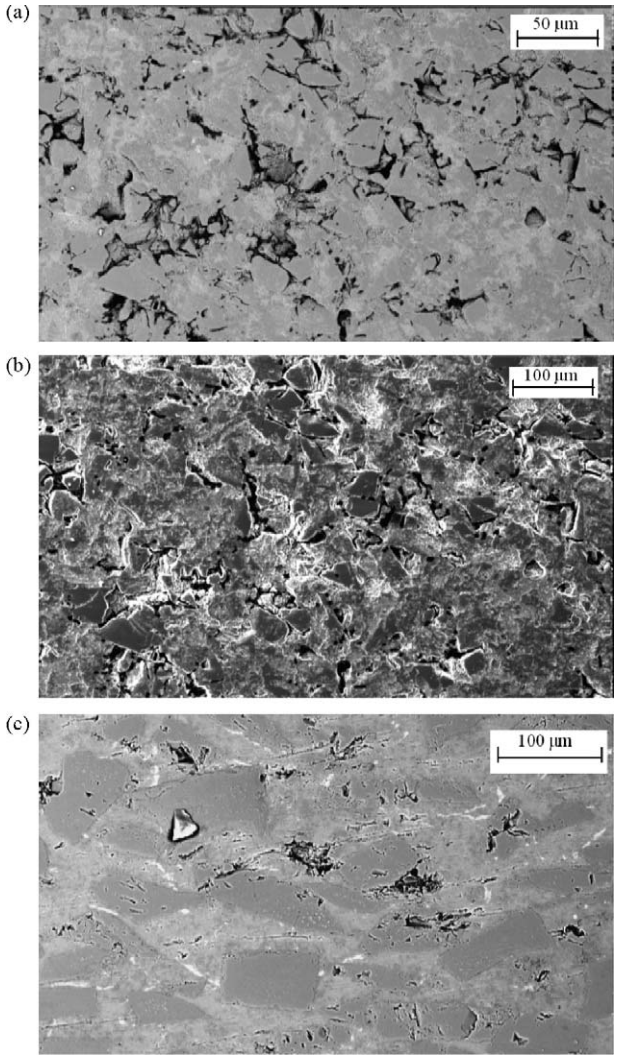

Fig. 6. Scanning electron micrographs (SEM) of composites fabricated based on the preforms with initial density of 0.4 theoretical density (TD) and with (a) 20 μm, (b) 50 μm, and (c) 90 μm SiC mean particle size.

Impact energies of composites fabricated based on the conditions reported in Table 2 (under MI1 condition) are shown in Fig. 7 as a function of preform fractional density. Final fractional density of the specimens is also added to the figure on each data point. As expected, preforms with a lower initial density have resulted to the composites with higher impact energies. The 0.4 TD dense preforms not only display the highest final densities but also the highest values of toughness in each diagram. The reason must be traced in two factors by which the impact energy can be seriously contributed. The first one is the final density of composites. The residual porosity in the microstructure of manufactured composites can be so detrimental to the mechanical properties that even a slight decrease in the residual porosity can lead to remarkable improvements of impact energy [12]. However, the essential parameter is the higher amount of tough phase in the final microstructure of composites fabricated based on the preforms with lower original density [24]. As can be calculated, while more than 55% of the open pores is filled by the molten aluminum in the 0.4 TD dense preform, this value has declined to less than 33% for the preforms with the initial density of 0.6 TD (90 μm SiC powder). The final volume fraction of tough phase (aluminum) in the composites with 0.4 TD dense preforms, therefore, is ∼22% higher than that in the composite with 0.6 TD dense preforms. This matter also holds true for the composites fabricated on the preforms made by 20 and 50 μm SiC powders.

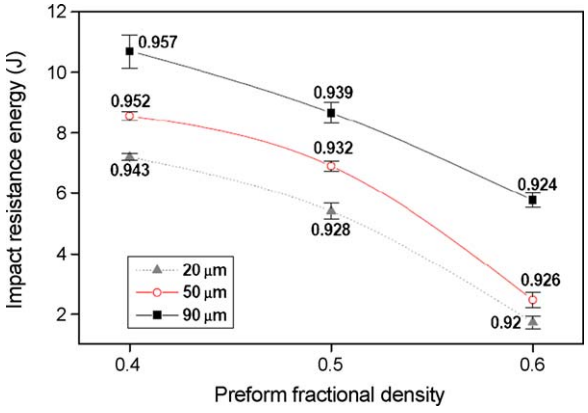

Fig. 7. Impact energy of the composites fabricated based on the SiC preforms with powder particle size of 20, 50, and 90 μm.

The other important feature, inferred in Fig. 7, is the enhancement of impact energy values with increasing particle size of the SiC powder. This may sound odd at the first glance because, as discussed in the literature, the lesser particle or grain size of the ceramic powder or ceramic body becomes, the higher fracture toughness would be obtained for that ceramic microstructure [25]. However, despite of a high-volume fraction of ceramics in such Al/SiC composites, their properties are, severely, depended on the ductile phase present in their microstructure. As explained above, larger particle size of the SiC powder generates thicker channels of pores in the SiC preforms. This ultimately leads to thicker Al channels in the final composite after the infiltration process [24]. The larger Al channels, consequently, provide higher value of impact energies for the composites produced by 90 μm SiC powder. Crack bridging by ductile metal ligaments is the most prominent mechanism to resist fracture and the dominant mechanism to dissipate the energy in the composite is plastic deformation through bridging ductile metal ligaments in the crack wake. In addition, the toughness improvement of a ceramic–metal composite is related to volume fraction of the ductile phase as well as the size and deformation behavior of the ductile channel [24,26]. Larger ductile channels or ligaments are capable of undergoing more plastic deformation by which more energy can be absorbed and the value of impact energy increases for coarser powders. The considerable issue is that closed values of composite densities resulted from higher infiltration times for finer particles (in return of equal initial density for preforms) allow a realistic determination of impact resistance for composites produced by different SiC particle size.

Fig. 8 depicts the impact energy of composites fabricated in different processing conditions of MI1, MI2, and MIS (Table 2). Density values of final composites yielded by

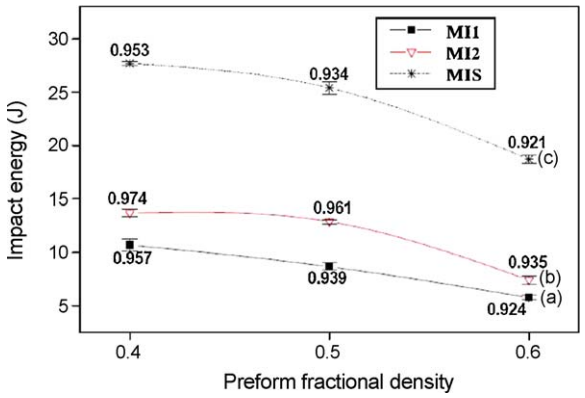

Fig. 8. Impact energy of the composites (90 μm SiC powder) fabricated by (a) melt infiltration at 950 °C (MI1), (b) melt infiltration at 1350 °C (MI2), and (c) melt infiltration at 950 °C followed by sintering at 1350 °C for 180 min in Ar atmosphere (MIS).

different processing conditions are also added to the figure. The higher value of final densities achieved by MI2 is attributed to the reduction of Al melt surface tension as well as the contact angle at ceramic–metal interface [9] with an increase in the infiltration temperature. The higher temperature can remove the oxide layer from the top of melt surface and thus, eases the infiltration of aluminum melt into the porous preforms [9]. Additionally, based on the calculations reported in the literature [1,11,12], at the temperatures higher than 1150 °C, formation of AlN phase is quite feasible through the reaction of aluminum vapor and the flowing nitrogen gas. The Al vapor pressure, at this temperature, is high enough to induce the gas phase reaction between the aluminum and nitrogen into the interstices of the porous preform. Formation of the AlN phase is, therefore, favorable in the process of filling the porosities by the molten aluminum [12]. Given by the mentioned reasons, MI2 must lead to higher final densities for obtained composites. As can be observed in Fig. 8, higher final densities of composites processed by MI2 created higher values of impact energy compared to those fabricated by MI1. In spite of a lower final density values displayed by the composites manufactured through the MIS method, they, interestingly, demonstrated the highest impact energies in comparison with infiltrated composites. To shed light on this consequence, SEM figures (Fig. 9) were provided from the interface of three kinds of composites. The fact is that the interface formation in a composite is principled on the diffusive mechanisms, the activation of which requires prolonged times and high-temperatures. Accordingly, the added sintering procedure (1350 °C for 3 h) after infiltration at 950 °C, favors the activation of diffusive mechanisms and thus, results to a good interface formation between the SiC and aluminum [27]. Fig. 9 confirms the accuracy of this issue by showing the SEM figures concerning with the interface of manufactured composites.

Fig. 10 demonstrates the XRD pattern of composites manufactured on the 0.6 TD initially dense preforms (90 μm SiC powder) using processing conditions in Table 2. As can be observed, the most obvious distinguishing parameter in the XRD patterns refers to the presence of AlN phase in the XRD

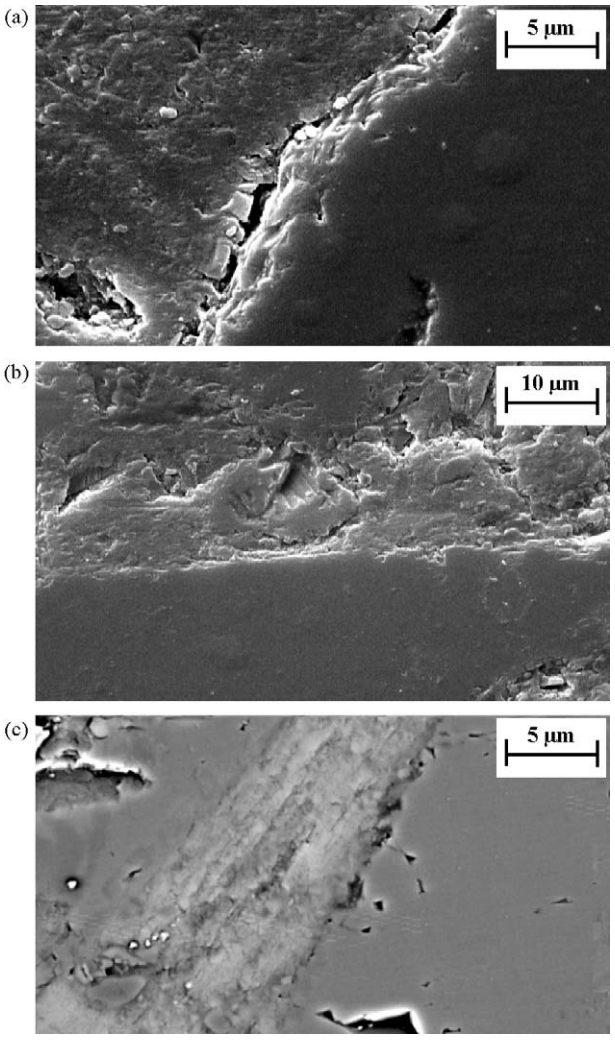

Fig. 9. Scanning electron micrographs (SEM) concerning with the interface of composites fabricated by (a) melt infiltration at 950 °C (MI1), (b) melt infiltration at 1350 °C (MI2), and (c) melt infiltration at 950 °C followed by sintering at 1350 °C for 180 min in Ar atmosphere (MIS).

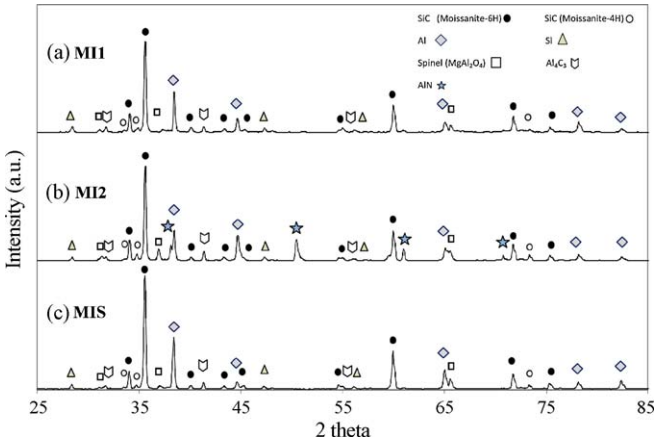

Fig. 10. The XRD pattern of composites fabricated by (a) melt infiltration at 950 °C (MI1), (b) melt infiltration at 1350 °C (MI2), and (c) melt infiltration at 950 °C followed by sintering at 1350 °C for 180 min in Ar atmosphere (MIS).

pattern related to MI2. In Fig. 10a, final microstructure of MI1-processed composite exposes no trace of AlN phase as a common product of melt infiltration. As the matter of fact, the applied infiltration temperature (950 °C) is not enough to result in AlN formation. Presence of aluminum nitride in the XRD pattern of composite provided by the MI2 procedure (Fig. 10b) confirms the mentioned issue about the necessary temperature for AlN formation. The fact is that the temperature range from 1150 to 1350 °C is the range through which aluminum nitride is thermodynamically stable and based on the experimental system, AlN can even remain stable up to higher temperatures [28,29]. The XRD pattern concerning with the MIS-processed composite (Fig. 10c), on the contrary, represents no phase other than those shown in Fig. 10a. In this sample the infiltration at 950 °C was followed by a sintering procedure in the neutral Ar atmosphere in which formation of AlN has not been observed. Other expected phases (Al_4C_3, $MgAl_2O_4$, etc.) are, however, observable in all XRD patterns. The other phase which is not detected in the patterns is Mg_2Si, the absence of which might be attributed to the lack of excessive free silicon phase in the powder or the alloy.

4. Conclusion

Pressureless melt infiltration process was applied in the current investigation to fabricate Al/SiC composites based on the SiC porous preforms. Results of the experiment revealed that composite final density rises with a decrease in the preform initial density and an increase in the SiC particle size. Both factors are capable of increasing hydraulic radius by which the threshold pressure of infiltration has an inverse relation. Additionally, the initial density of preforms was found to be a more effective parameter to progress the melt infiltration process rather than the SiC particle size. The impact resistance tests revealed the improvement of impact energies as a result of reduction in preforms initial density (SiC volume fraction). The reason lies in the higher volume fraction of aluminum as the ductile phase, in addition to the lower value of residual porosity in the final microstructure of composites fabricated on the lower initially dense preforms. The other conclusion is the improvement of impact energy with an increase in SiC mean particle size. Larger Al channels in the microstructure of composites fabricated by 90 μm SiC powder withstand more plastic deformation and provide composites with higher impact energies. Additionally, composites manufactured by combined melt infiltration and sintering procedure enjoy the highest values of impact energies in comparison with infiltrated ones. Microstructural observations confirm that such an effect is attributed to a good interface formation and stronger ceramic–metal ligaments in the contact regions of SiC and aluminum alloy which is due to a longer time for activation of diffusive mechanisms at the interface region.

Acknowledgments

The authors of this article express their profound gratitude to Mr. M. Haghighatzadeh, Mr. M.M. Hejazi, and Mr. M.H. Shaeri for their precious cooperation during the course of this research. The authors also appreciate valuable services made by all personnel of Iran University of Science and Technology (IUST).

References

[1] M.I. Pech-Canul, M.M. Makhlouf, J. Mater. Synth. Process. 8 (2000) 35–53.
[2] C. Garcia-Cordovilla, E. Louis, J. Narciso, Acta Metall. 47 (1999) 4461–4479.
[3] E. Candan, H.V. Atkinson, H. Jones, Scripta Mater. 38 (1998) 999–1002.
[4] A. Zulfia, R.J. Hand, J. Mater. Sci. 37 (2002) 961–995.
[5] E. Candan, H.V. Atkinson, H. Jones, J. Mater. Sci. 35 (2000) 4955–4960.
[6] E. Candan, H.V. Atkinson, H. Jones, J. Mater. Sci. 32 (2000) 289–294.
[7] E. Candan, Mater. Lett. 60 (2006) 1204–1208.
[8] E. Ahlatci, E. Candan, H. Cimenoglu, Metall. Mater. Trans. A 35 (2003) 2127–2141.
[9] J. Tian, E. Pinero, H. Narciso, E. Louis, Scripta Mater. 53 (2005) 1483–1488.
[10] G.P. Martins, D.L. Olson, G.R. Edwards, Metall. Mater. Trans. B 19 (1988) 95–103.
[11] M.I. Pech-Canul, R.N. Katz, M.M. Makhlouf, J. Mater. Process. Technol. 108 (2000) 68–77.
[12] F. Ortega-Celaya, M.I. Pech-Canul, M.A. Pech-Canul, J. Mater. Process. Technol. 183 (2007) 368–373.
[13] B.C. Pai, G. Ramani, R.M. Pillai, K.G. Satyanarayna, J. Mater. Sci. 30 (1995) 1903–1910.
[14] M.I. Pech-Canul, R.N. Katz, M.M. Makhlouf, Metall. Mater. Trans. A 31 (2000) 565–573.
[15] K. Aoki, O. Izumi, Nipp. Kinz. Gakk. 43 (1979) 1190–1196.
[16] C.T. Lui, C.L. White, J.A. Horton, Acta Metall. 33 (1985) 213–229.
[17] K.P. Plucknett, P.F. Becher, K.B. Alexander, J. Microsc. 185 (1997) 206–216.
[18] K.P. Plucknett, P.F. Becher, R. Subramanian, J. Mater. Res. 12 (1997) 2515–2517.
[19] R. Subramanian, J.H. Schneibel, K.B. Alexander, K.P. Plucknett, Scripta Mater. 35 (1996) 583–588.
[20] P. Plucknett, T.N. Tiegs, P.F. Becher, U.S. Pat. No. 5,905,937 (May 18, 1999).
[21] P. Plucknett, T.N. Tiegs, P.F. Becher, S.B. Waters, P.A. Menchhofer, Ceram. Eng. Sci. Process. 17 (1996) 314–321.
[22] K.P. Plucknett, P.F. Becher, J. Am. Ceram. Soc. 84 (2001) 55–61.
[23] R.C. Carman, Soil Sci. 52 (1941) 1–9.
[24] S.R. Boddapati, J. Rodel, V. Jayaram, Composites A 38 (2007) 1038–1050.
[25] A. Krell, P. Blank, J. Eur. Ceram. Soc. 16 (1996) 1189–1200.
[26] N. Nagendra, B.S. Rao, V. Jayaram, Mater. Sci. Eng. A 269 (1999) 26–37.
[27] B.S. Murty, S.K. Thakur, B.K. Dhindaw, Metall. Mater. Trans. A 31 (2000) 319–325.
[28] Q. Zheng, R.G. Reddy, J. Mater. Sci. 39 (2004) 141–149.
[29] Q. Zheng, R.G. Reddy, Metall. Mater. Trans. B 34 (2003) 793–804.